

Research Article

Biosynthesis of Gold Nanoparticles using *Osmundaria Obtusiloba* Extract and their Potential use in Optical Sensing Applications

Rojas-Pérez A¹, Adorno L², Cordero M³, Ruiz A³, Mercado-Díaz Z¹, Rodríguez A⁴, Betancourt L¹, Vélez C¹, Feliciano I¹, Cabrera C¹ and Díaz-Vázquez LM^{1*}

¹Department of Chemistry, University of Puerto Rico-Rio Piedras Campus, Puerto Rico

²Nutrition Program, University of Puerto Rico-Rio Piedras Campus, Puerto Rico

³Interdisciplinary Program, University of Puerto Rico-Rio Piedras Campus, Puerto Rico

⁴Department of Environmental Science, University of Puerto Rico-Rio Piedras Campus, Puerto Rico

*Corresponding author: Díaz-Vázquez LM, Chemistry Department, University of Puerto Rico, Rio Piedras, PO Box 23346, San Juan, P.R. 00931, Puerto Rico

Received: September 02, 2015; Accepted: September 26, 2015; Published: September 29, 2015

Abstract

The optical properties of gold nanoparticles depend on particles size, shape, protective ligand and the synthesis method used for their production. The present study describes an eco-friendly method for the synthesis of gold Nanoparticles (AuNPs) utilizing the macro algae *Osmundaria Obtusiloba*. The optical properties of the obtained nanoparticles and whether the use of the macroalgae extract confers them with additional properties were evaluated and compared with nanoparticles obtained via traditional methods. AuNPs were physical and chemically characterized by UVVIS, FTIR, HRTEM, SEM-EDS, XRD and Raman Spectroscopy. The UVVIS spectra showed a peak at 540 nm that confirmed the formation of AuNPs. XRD pattern confirmed a face centered cubic (*fcc*) crystalline structure for these nanoparticles. HRTEM images revealed several shapes including spherical, triangular, and diamond shaped nanoparticles with size ranges between 10 to 20 nm. The presence of 83.58 %wt. of elemental Au in the obtained nanoparticles was elucidated via EDS. Synthesized AuNPs SERS enhancement factor toward 4-nitrothiophenol concentration determination. Additionally, their utility as fluorescence quencher or enhancer was evaluated using methyl orange.

Keywords: Gold Nanoparticles; Biosynthesis; *Osmundaria Obtusiloba*; SERS; Fluorescence enhancement and quenching

Abbreviations

AuNPs: Gold Nanoparticles; UVVIS: Ultraviolet-Visible; SERS: Surface Enhanced Raman Spectroscopy; PL: Photoluminescence; AuNPs-Osm: Gold Nanoparticles Synthesized with *Osmundaria Obtusiloba* extract; AuNPs-NaBH₄: Gold Nanoparticles Synthesized with NaBH₄; SPR: Surface Plasmon Resonance; MO: Methyl Orange; FTIR: Fourier transform infrared spectroscopy; HR-TEM: High Resolution Transmission Electron Microscopy; SEM-EDS: Scanning Electron Microscopy- Energy Disperse Spectroscopy; XRD: X-Ray Diffraction; AEF: Analytical Enhancement Factor; NR: Normal Raman

Introduction

Gold Nanoparticles (AuNPs) have widely been used as an essential element in the fabrication of sensing and electronic devices, as well as for biomedical applications, because of their remarkable physical and chemical properties [1-5]. The use of AuNPs in spectrometric analysis is related to their Surface Plasmon resonance (SPR) properties, which cause that its solutions display a range of colors from red, purple, to violet with increasing particle size. This color is related to the strong absorption and scattering of radiation at 520 nm, which is the result of the collective oscillation of conduction electrons on the surface of AuNPs when they are excited by the incident light [6]. AuNPs SPR properties depend on particles size, shape, protective ligand, refractive index of the solvent, and temperature. Also AuNPs can enhance Raman radiation scattering, which leads to

the development of Surface Enhance Raman Spectroscopy (SERS) based sensing. AuNPs can enhance or quench the fluorescence of a fluorophore depending on the AuNP-fluorophore distance [7]. All these mentioned AuNPs optical properties can be tailored during the synthesis of the nanoparticles through inducing a change in their size, morphology, and surface modifications.

During the last decade, many research efforts have been focused on the development of AuNPs's synthesis methods to tailor their physical and chemical properties in order to expand their use for different research and industrial applications. Wet methods of synthesis are a bottom-up process in which the nanoparticles are produced by reducing gold salts in the presence of appropriate capping agents that minimize particle aggregation. The method proposed by Turkevich and coworkers in 1951, in which tetrachloroauric acid (HAuCl₄) is reduced in water by sodium citrate, and the reduction of gold salts with Sodium Borohydride (NaBH₄) have been the most popular methods [8,9]. The top-down methods are used to produce AuNPs from bulk material via mechanical and/or physical processes to reduce it to the desired size such as milling, laser ablation [10], and digestive ripening [11].

Although there are a variety of AuNPs synthesis methods, they are fraught with many problems including the use of toxic solvents, generation of hazardous by-products, and high energy consumption [5]. Alternative routes for metallic nanoparticle synthesis stem from the use of natural resources in order to provide a cost effective and environmentally method [12]. Simple prokaryotes to complex

eukaryotic organisms, including higher angiospermic plants, are being used for the production of low-cost, energy-efficient, and nontoxic metallic nanoparticles [13]. Particular interest is given to the use of plants as a natural resource in the biosynthesis of metallic nanoparticles. Plants polyphenols, proteins, carbohydrates and other biomolecules allow them to act as reducing and stabilizing agents in nanoparticles synthesis [14,15].

The use of macroalgae is being researched as a possible new natural resource for AuNPs biosynthesis. Marine macroalgae are known as biofactories, because they are a rich source of biologically active compounds and antioxidants such as polyphenols, bromophenols, polysaccharides, photosynthetic pigments, proteins, vitamins, fatty acids, glycolipids, and protective enzymes [16]. Although macroalgae, like other photosynthesizing organisms, are constantly exposed to environmental conditions that lead to the formation of free radicals and other oxidizing agents, they are resilient to oxidative damage to their structural components. Their resistance to oxidation during photosynthesis and storage suggests that their cells have developed protective antioxidative defense systems [17]. Consequently, macroalgae chemical composition enables them to act as reducing and stabilizing agents in nanoparticles synthesis similarly to plants. The use of macroalgae extract could thus provide us with an ecofriendly and cost effective new method to synthesize metallic nanoparticles.

This research was directed towards determining whether the use of the macroalgae *Osmundaria Obtusiloba*, obtained from the north coast of Puerto Rico, is an appropriate resource to mediate the biosynthesis of AuNPs. Additionally, these biosynthesized nanoparticles were compared with nanoparticles synthesized using sodium borohydride as a reducing agent, in order to evaluate if the implementation of the macro algae extract provoked changes in functionality and/or the optical properties of the nanoparticles. The obtained nanoparticles were subjected to characterization methods in order to determine their size, composition, and morphology. The SERS enhancement properties of AuNPs produced via both synthesis methods were determined and compared. In addition AuNPs utility as a fluorescence enhancer or quencher was evaluated using Methyl Orange (MO) as a model compound.

Materials and Methods

Materials

Hydrogen Tetrachloroaurate (III) trihydrate ($\text{HAuCl}_4 \cdot 3\text{H}_2\text{O}$) 99.9 +%, sodium borohydride, methyl orange, and 4-nitrothiophenol (80%) were purchased from Sigma Aldrich and were used as received. All the glassware was analytically washed with sulfuric acid and nitric acid followed by nanopure water. All the solutions were prepared using nanopure water (18.2M Ω .cm) obtained from a Barnstead Nanopure Diamond™.

Preparation of macroalgae biomass and extract

The macroalgae *Osmundaria Obtusiloba* was collected from the north coast of Puerto Rico. It was washed and cleaned with distilled water to remove epiphytes and detritus attached to it. Then, it was dried at 65 °C, pulverized, sieved through < 0.5 mm, and stored at room temperature in a desiccator. A macroalgae extract was prepared by boiling 5.00g of grinded macroalgae in 100mL of anethanolic solution

(1:1 ethanol and nanopure water) at 70°C for 20 min. The mixture was transferred to centrifuge tubes and subjected to 2,000 rpm for 20 minutes; the supernatant was filtered, evaporated to dryness, and reconstituted in nanopure water. The extract was characterized by UVVIS and FTIR spectroscopy, and stored at 4°C for further use.

Biosynthesis of Gold Nanoparticles

An aqueous solution of 1mM HAuCl_4 was prepared. Reaction mixtures containing 5.0 mL of the algae extract and 20.0 mL of 1mM HAuCl_4 were incubated at 60 °C, under a constant agitation of 200 rpm, for 2 hours. Changes in color of the reaction mixture were used to indicate the formation of nanoparticles. Aliquots of the reaction mixture were analyzed, using a UVVIS spectrophotometer (Hach Dr5000) with a resolution of 1 nm, every five minutes in order to determine whether nanoparticle formation had occurred by observing the absorbance at the characteristic band for AuNPs near 520 nm. In order to collect and purify the produced nanoparticles, the reaction mixture was centrifuged at 20,000rpm for 20 min, the precipitate was collected, and the supernatant was again centrifuged at 20,000rpm for 20 min. The collected solid pellets were washed with high purity ethanol to remove residues from the macroalgae extract and centrifuged at 20,000 rpm for 15 min. The supernatant was removed and the pellet was dried at 65°C under an inert nitrogen flow. The dried AuNPs were stored in desiccators for further analysis.

Chemical synthesis of AuNPs using NaBH_4

AuNPs were synthesized using NaBH_4 as the reducing agent using the methodology suggested by Mulfinger, L. et al. [9]. Briefly, an aliquot of 10.00 mL of 1.0 mM Gold (III) chloride hydrate was added dropwise (approximately 1 drop per second) to 30 mL of a 2.0 mM NaBH_4 solution that had been chilled in an ice bath. The reaction mixture was stirred vigorously on a magnetic stir plate. The solution turned violet after the addition of 1 mL of gold solution. After the entire addition, the stirring was stopped, the stir bar removed, and the resulting solution stored for further use. The nanoparticles were recovered with the same procedure used for AuNPs biosynthesized with *O. Obtusiloba* extract.

Characterization of AuNPs

The size and morphology of AuNPs were evaluated using High Resolution Transmission Electron Microscopy (HRTEM) and Scanning Transmission Electron Microscopy (STEM). The analyses were done using a FEI Tecnai F20 microscope with a monochromator-energy filter. An 80 mm Oxford SDD detector was used for X-ray detection, and the images were analyzed using the Inca Software. Samples for HRTEM were prepared by drop-coating AuNPs solution onto carbon-coated copper grids. The crystal nature of AuNPs was determined by X-Ray Diffraction (XRD) analysis using a Rigaku ULTIMA III Diffractometer with a Cu-K_α radiation source ($\lambda = 1.5406 \text{ \AA}$) operating at 40 kV and 44 mA. The XRD patterns were recorded between 30° and 90° at scan rate of 4.0°/min. Gold concentration, conversion, and composition of nanoparticles were determined using disperse SEM-X-ray fluorescence spectrometer and Energy Dispersive Spectroscopy (EDS) at 20kv under 5,000x magnification with a Bruker S4 Pioneer Instrument. The presence of functionalization of the AuNPs surface was evaluated by Attenuated Total Reflectance-Fourier Transform Infrared Spectroscopy (ATR-FTIR) The ATR-FTIR spectra were recorded at a resolution of 1 cm^{-1}

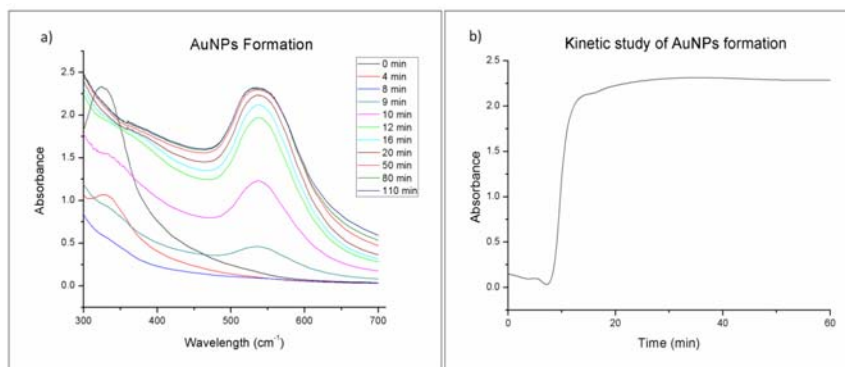


Figure 1: a) UV-Vis Spectra for the biosynthesis reaction mixture at different times; b) Absorbance at 540 nm at different reaction times for the biosynthesis of AuNPs with *O. Obtusifoloba* extract.

¹between 300 and 4000 cm⁻¹ at a Shimadzu IRAffinity-1 with an ATR 8000A accessory.

Optical properties of AuNPs

UV-Visible spectra of the AuNPs solution was recorded using a UV-VIS spectrophotometer (Hach Dr5000) with a resolution of 1 nm over a wavelength range of 250 to 750 nm using 1 cm path length quartz cuvettes. These cuvettes were cleaned before each use by sonicating them for five minutes in an acidic solution (H₂SO₄ 0.10 M) and then rinsed with deionized water until the pH of the effluent was 7.0. The UV-spectra were used to compare the AuNPs in terms of their SPR properties and estimated the size using the peak maxima. For each type of AuNPs, UVVIS spectra at five different concentrations were recorded by directly diluting the as-prepared nanoparticles solution with nanopure water to the expected concentrations [18].

Quantum yield

The quantum yield of the synthesis AuNPs was determined using a procedure reported by Fery&Lavabre, 1999 [19]. Quinine sulfate acidic solution (0.05 M H₂SO₄) was used as a reference standard, for which quantum yield is $\eta_{\text{yield}} = 0.54$ at an emission range 400-600 nm as reported in the literature. Absolute values of the quantum yield were calculated using the following equation (1)

$$\Phi_x = \Phi_{\text{std}} \left(\frac{I_x}{A_x} \right) \left(\frac{A_{\text{std}}}{I_{\text{std}}} \right) \left(\frac{\eta_x^2}{\eta_{\text{std}}^2} \right) \quad (1)$$

Where the Φ_x is the quantum yield of the AuNPs and Φ_{std} of Quinine sulfate, A is the absorbance at the emission wavelength, I is the area under the corrected emission curve wavelength, and η is the refractive index of the solvent of the corresponding solution. To reduce the reabsorption within the sample on the observed emission spectrum, the absorbance values of all the solutions were maintained under 0.05 [19,20].

Fluorescence properties

The effects of AuNPs synthesized with *O. Obtusifoloba* on the fluorescence properties of Methyl Orange (MO) were studied and compared with the effect of AuNPs synthesized with NaBH₄. All the analyses were performed in a Shimadzu RF-5301 Spectrophotofluorometer, using medium scanning speed, high sensitivity, and excitation and emission slit widths of 10 nm. After each sample run, the fluorometer quartz cuvettes were rinsed with

sulfuric acid and distilled water until the effluent had a neutral pH and dried prior use with the next sample.

A 10 μ M stock solution of methyl orange was prepared and adjusted to pH 4.0 with phosphate buffer solution. A set of aqueous solution was prepared for each type of NPs, maintaining the MO concentration constant at 1 μ M and varying the concentration of nanoparticles from 0.17 mg/L to 17.9 mg/L. For each solution, the emission spectra were recorded using an excitation wavelength of 270 nm and an emission range of 250 to 800 nm.

Surface enhancement raman spectroscopy (SERS) enhancement

The SERS enhancement of the AuNPs toward 4-Nitrothiophenol (4-NTP) was evaluated and compared with SERS of Au-NPs synthesized with NaBH₄. For this purpose, the procedure reported by Seongmin Hong and Xiao Li was followed [21]. Briefly, 4-NTP samples were prepared using 1.00 mL of gold colloidal solutions with different amounts of 4-NTP, ranging from 0.1 to 0.7 μ M, then 1.00 mL of 1M NaCl was added to all solutions. The concentration of gold nanoparticles was kept constant for all solutions. All the SERS experiments were carried out using Raman Microscopy (Thermo Scientific, DXR), an excitation laser with a wavelength of 780 nm was applied with 10 mW of power, 3 s of exposure time, and 3 accumulations. The spectrum grating was 700, and a 20X microscopic objective lens were used for the analysis. All the reported analyses were performed three times. Prepared samples were maintained in darkness for 10 minutes prior to the analysis to minimize fluctuations of SERS spectra by allowing the solutions to reach an equilibrium state. The SERS Analytical Enhancement Factor (AEF) was calculated using equation (2) as reported by Seongmin, where I_{SERS} and I_{NR} are the intensity of the selected vibrational peak in SERS and Normal Raman (NR) measurements, respectively, and C_{NR} and C_{SERS} are the concentration of 4-NTP used for NR and SERS measurement, respectively.

$$EF = \frac{I_{\text{SERS}} C_{\text{NR}}}{I_{\text{NR}} C_{\text{SERS}}} \quad (2)$$

Results

Biosynthesis and chemical synthesis of AuNPs

The synthesis of gold nanoparticles using *Osmundaria Obtusifoloba*

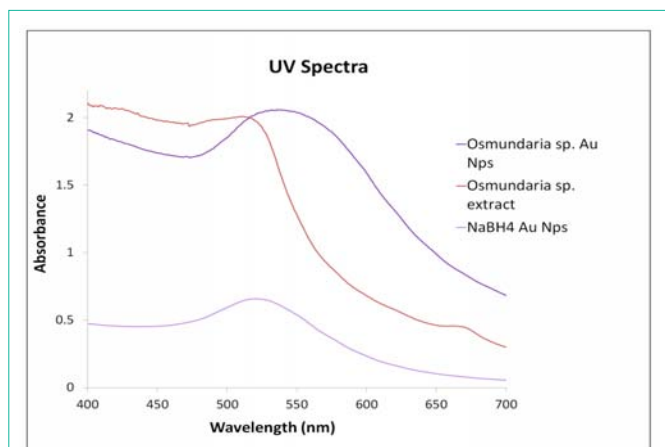


Figure 2: UV-Vis spectra of macro algae *Osmundaria Obtusiloba* extract, macro algae synthesized gold nanoparticles and NaBH_4 gold nanoparticles.

extract (AuNPs-Osm) was done successfully, as confirmed by the distinct color appearance and UVVIS spectrophotometric data. The SPR band of the reaction mixture was kinetically monitored from 300 to 750 nm. Initially, the reaction mixture exhibit a band near 325 nm, characteristic of the *O. Obtusiloba* extract as shown in Figure 1a; however, as the reaction proceeded, this band decreased, while a band centered at around 540 nm (characteristic of the SPR of AuNPs) was revealed and became more pronounced with time. This tendency confirms that the macroalgae extract is acting as a reducing and capping agent in the biosynthesis of AuNPs. Our results showed that the reaction was completed in approximately 20 minutes (Figure 1b), afterwards reaching a steady state. After recovering the synthesized nanoparticles, a 92% yield was determined by gravimetric analysis. The expounded results confirm that the biosynthesis method is time-suitable and efficient.

The chemical synthesis of AuNPs using NaBH_4 was also done successfully and confirmed by color change and the appearance of the characteristic UVVIS absorption band near 530 nm. This SPR band corresponds to the formation of small and spherical gold nanoparticles. The AuNPs formed with *O. Obtusiloba* extract showed a broader and red shifted SPR band at 540 nm. This may be attributed to the formation of larger anisotropic nanoparticles [22,23]. Figure 2 compares the UVVIS spectra obtained for AuNPs obtained by both methods. Both wavelength values for the SPR bands have been reported in previous studies indicating the presence of gold nanoparticles. Fernando et al. reported the absorbance peaks of gold nanoparticles at 570 and 541 nm [24], correlating excellently with the aforementioned results.

Characterization

XRD studies were carried out to confirm the crystalline nature of Au nanoparticles. The performed analysis was used for phase and diffraction pattern identification of AuNPs synthesized by biochemical reduction using the macroalgae *O. Obtusiloba* (AuNPs-Osm). Figure 3 shows the diffraction pattern consisted of five peaks at 38.2° , 44.3° , 64.6° , 77.5° , and 81.6° corresponding to the AuNPs (111), (200), (220), (311), and (222) planes, respectively. These results demonstrated that has a face centered cubic (fcc) crystalline structure. The average particle size for each plane calculated using the Scherer

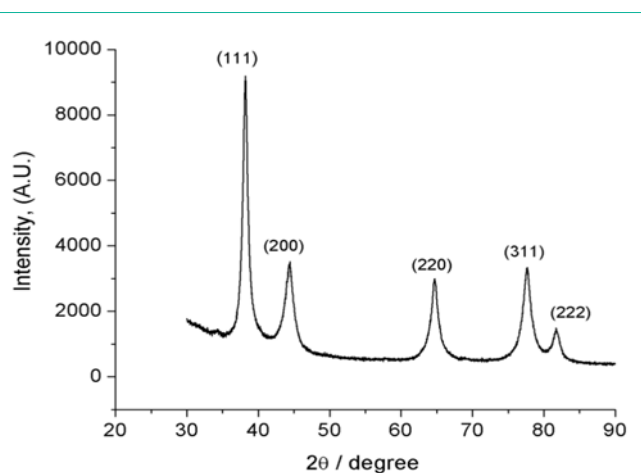


Figure 3: XRD patterns of AuNPs biosynthesized with *Osmundaria Obtusiloba* extract.

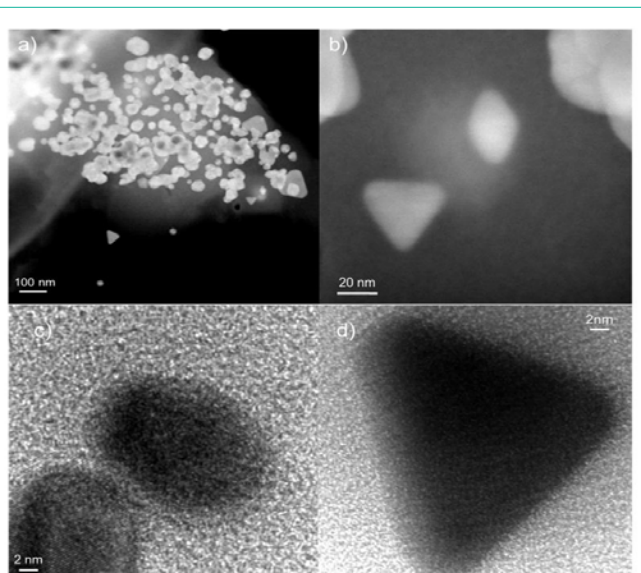


Figure 4: (a-b) Scanning transmission electron microscopy of AuNPs-Osm and (c-d) high resolution transmission electron microscopy of AuNPs reduced with algae extract.

equation, was between 6 nm and 10 nm for the different crystalline planes.

TEM was used to provide valuable information about particle size, shape, and average dispersion. Figure 4 (a-b) presents STEM images evidencing well dispersed, very small isolated nanoparticles, which appear as bright dots, corresponding to a high Z element. HR-TEM images in Figure 4(c-d) shows as-prepared AuNPs, after the reduction using algae extract. Interestingly, these nanoparticles possess different shapes including spherical, triangular, diamond, and hexagonal shapes with an approximate particle size of 10 nm, supported by XRD data. Agglomerated AuNPs were also observed in the samples. Remarkable differences in particle morphologies were found, which was unexpected from the synthetic process. HRTEM was used to isolate single particles and show their shapes, size, and lattice. The presence of Au was further confirmed in Figure 5, which displays the EDS analysis of these AuNPs.

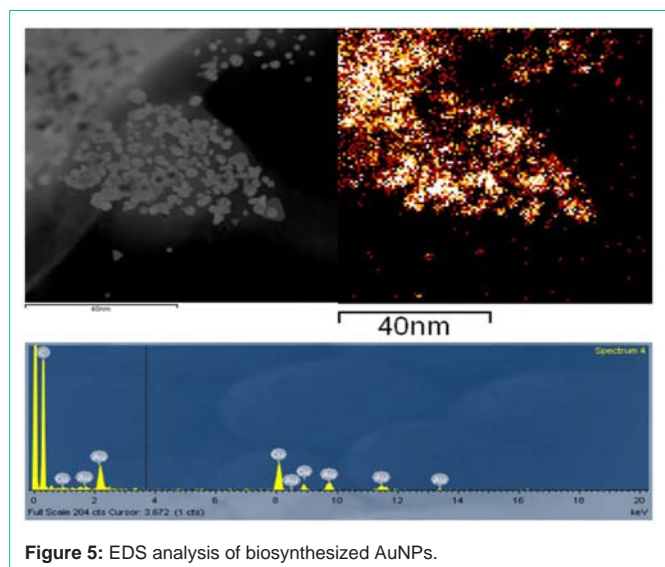


Figure 5: EDS analysis of biosynthesized AuNPs.

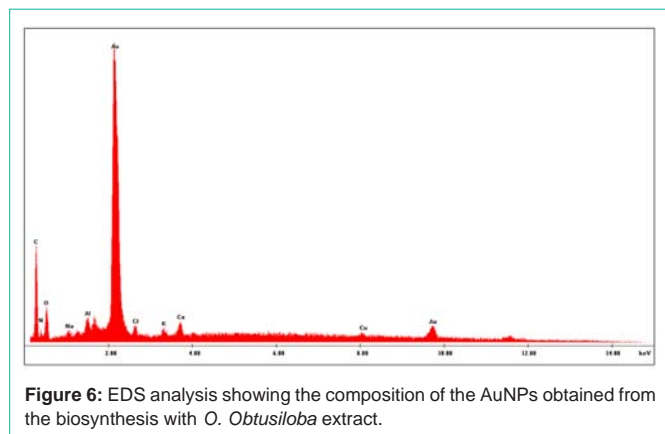


Figure 6: EDS analysis showing the composition of the AuNPs obtained from the biosynthesis with *O. Obtusiloba* extract.

The presence of 83.58 %wt. of elemental gold in the obtained nanoparticles was also confirmed by EDS. Table 1 and Figure 6 present EDS quantitative results obtained when samples of dried AuNPs-Osm were analyzed. The values obtained for percent by weight (Wt%) confirms the presence of other elements such as Mg, Na, Cl, Ca, and K, which are common in the macroalgae biomass, however,

Table 1: EDS Quantitative Analysis of AuNPs synthesized with macro algae extract (20kV, 5,000x).

Element	Wt%	At%
CK	9.90	51.15
NK	2.06	9.14
OK	2.26	8.76
FK	0.13	0.43
NaK	0.17	0.47
MgK	0.09	0.23
AlK	0.86	1.98
ClK	0.30	0.53
KK	0.16	0.26
CaK	0.48	0.74
AuL	83.588	26.33

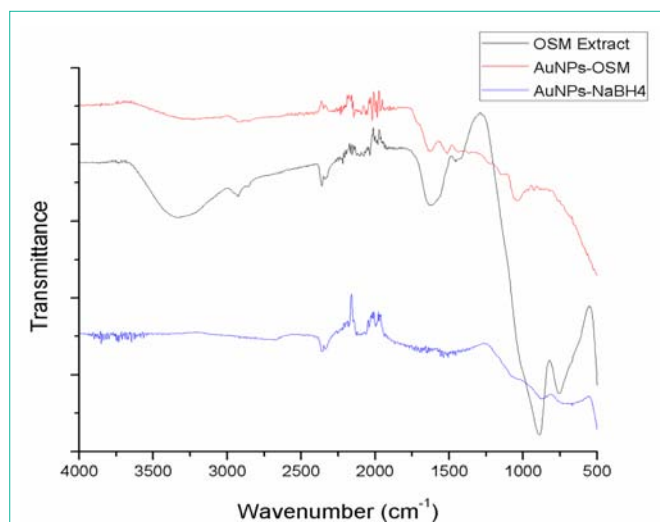


Figure 7: ATR-FTIR absorption spectra of AuNPs-*Osmundaria*, *Osmundaria Obtusiloba* Extract prior to the synthesis, *Osmundaria Obtusiloba* Extract after the reaction, and AuNPs-NaBH₄.

Auremainedthe major component of the obtained nanoparticles.

The interaction of AuNPs with the biomolecules of the *O. Obtusiloba* extract was evaluated through the ATR-FTIR analysis of the dried powder of the synthesized nanoparticles and the macroalgae extracts. The FTIR analysis was used to identify the biomolecules or compounds in *O. Obtusiloba* responsible for the reduction and efficient stabilization of the bio-reduced gold nanoparticles. Figure 7 presents the ATR-FTIR spectrums for *Osmundaria Obtusiloba* extract, AuNPs-Osm, and AuNPs-NaBH₄. *Osmundaria Obtusiloba*'s extracts exhibit characteristic peaks indicating the presence of functional groups at 3346 cm⁻¹, 1650 cm⁻¹, 1602 cm⁻¹, 910 cm⁻¹ and 750 cm⁻¹. The bands at 3346 and 910 cm⁻¹ correspond to alcohol functional groups. These bands may be attributed to the presence of polyphenols, polysaccharides, and other alcohols in the macro algae extract. The peak at 1650 cm⁻¹ corresponds to a carbon double bond stretch (C=C), and the peak at 750 cm⁻¹ corresponds to a carbon-hydrogen bond. The FTIR spectrum of AuNPs-Osm, shows some small peaks at 1630 cm⁻¹, 1504 cm⁻¹, and 1029 cm⁻¹. The FTIR of the macroalgae extract previous to the nanoparticle synthesis shows a peak at 1650 cm⁻¹, which was shifted to a lower wavelength (1630 cm⁻¹) after the synthesis. This indicates that this functionality is participating as a capping agent in the reduction of Au³⁺ to Au⁰. A similar behavior was observed with the hydroxyl groups. The presence of these bands in the algae extract can be attributed to some of the constituents of macro algae: terpenoids (1650 cm⁻¹) and extracellular polysaccharides (3346 cm⁻¹). The macroalga *O. Obtusiloba* has a high content of extracellular polysaccharides that may be acting as stabilizing agents for the AuNPs, minimizing their agglomeration. Recent studies have reported similar findings in which the presence of carboxylic, amine, and alcohol groups were associated with the algae-assisted synthesized gold nanoparticles [25,26]. In the case of the AuNPs prepared with sodium borohydride, no characteristic peaks related to organic compounds were detected Figure 7.

Optical properties of AuNPs-Osm

The optical properties of AuNPs, such as absorption and

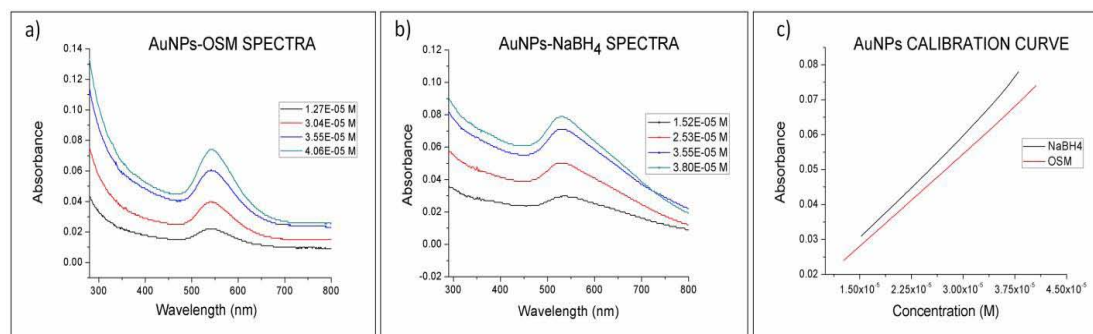


Figure 8: a) UV-Vis spectra for AuNPs-*Osmundaria* and b) AuNPs- NaBH_4 at different concentrations. c) Absorbance at the SPR band as a function of the nanoparticle concentration (540nm AuNPs-*Osmundaria*, 530nm AuNPs- NaBH_4).

emission maxima, are particle size dependent. Figure 2 shows the variation in absorbance capacity of AuNPs with the synthesis method implemented. As mentioned previously, for the AuNPs-Osm the maximum extinction of SPR band was shifted from the expected 520 to 540 nm. This behavior may be ascribed to the surface plasmon oscillation of free electrons. In the case of the AuNPs- NaBH_4 , a smaller shift was observed from 520 to 530 nm. According to Mie theory, the red shift of the SPR band increases with the particle size [23], which is in accordance with the TEM results, showing larger particles for the biosynthesis method (10-20 nm). This difference however, may not be due only to their size, but also to differences in morphology. While NaBH_4 reduction produces spherical nanoparticles with a size from 6 to 20 nm, the algae-based synthesis generated a varied combination of morphologies: triangles, spheres, diamonds, and hexagonal shapes.

Figure 8 shows the variation in the absorbance of the AuNPs-Osm and AuNPs- NaBH_4 with concentration. For both types of nanoparticles, the absorbance was found to be proportional to the concentration of the solution. But nanoparticles prepared by chemical synthesis revealed to be more sensitive to absorption. This correlation between the concentration and the absorbance of the nanoparticles was expected, since an increase in the number of nanoparticles also increases the total surface available for the SPR [27].

In order to compare the Photoluminescence (PL) properties of the nanoparticles obtained via both methods used in this study, fluorescence spectra of the nanoparticles were obtained with an excitation wavelength of 270 nm and an emission range from 300 to 700 nm. The fluorescence spectrums for both types of nanoparticles,

AuNPs-Osm and AuNPs- NaBH_4 , have their maxima at 550 nm (Figure 9). The position of the photoluminescence band indicates that both types of gold nanoparticles exhibit high efficient single photon-induced luminescence. It may be associated to their ability to sustain resonating surface Plasmon's with negligible damping [15]. This spectrum also shows that the PL emission peak and UVVIS absorption band have their maxima at almost the same wavelength. This can lead to visible luminescence of gold nanoparticles.

Quantum yield

The quantum yields of the produced nanoparticles were determined using quinine sulfate as a reference standard and 310 nm as the excitation wavelength. A photoluminescence quantum yield of 3.0% for AuNPs-Osm and 2.0% for AuNPs- NaBH_4 were obtained. These values compare with previously reported values for Au nanoclusters and polymer-stabilized gold clusters [28,29]. Photoluminescence efficiency tends to decrease with an increase in the size of nanoparticles, but there is also evidence that other factors such as clustering, surface modification, and stabilizing interactions with the media can influence the exhibited fluorescence [30,31].

Fluorescence

Studies involving the quenching and enhancement of fluorescence adsorbed or closed to metal nanostructures provide valuable information about the interactions of the target fluorophores with metal nanostructures and the photoluminescence mechanism. The utility of the synthesized nanoparticles to enhance or quench the fluorescence signal of other molecules was evaluated using methyl

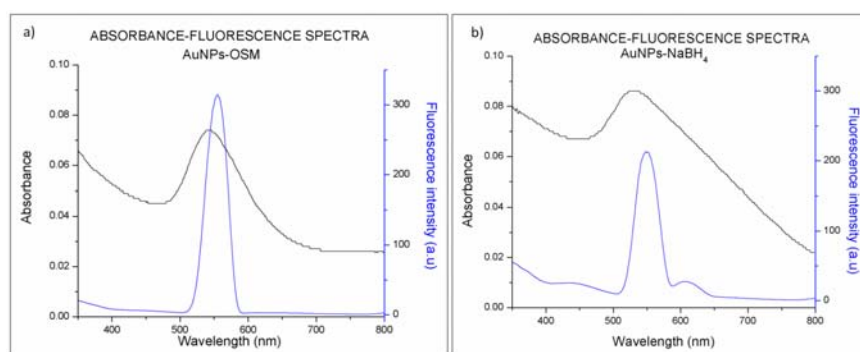


Figure 9: UV-Vis absorption and fluorescence emission spectra of a) AuNPs-*Osmundaria* and b) AuNPs- NaBH_4 .

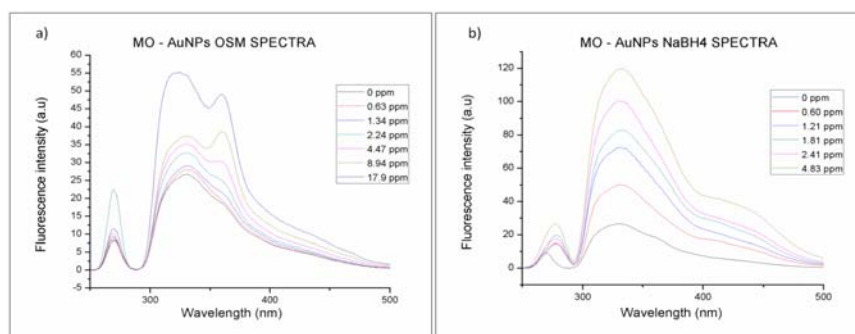


Figure 10: Fluorescence emission spectra of methyl orange solutions at pH 4, with different gold nanoparticles concentrations; a) AuNPs-*Osmundaria* and b) AuNPs-NaBH₄ (λ excitation= 270nm).

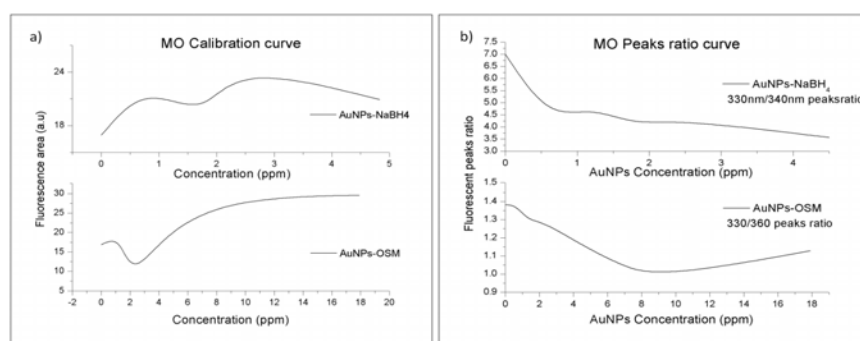


Figure 11: a) Integral fluorescence intensity of the 300-500 nm band and for MO as a function of the AuNPs concentration. b) Fluorescence intensity ratio of the peak centered at 330 nm and its shoulder as function of the AuNPs concentration. (λ excitation= 270 nm, pH=4.0).

orange as the model molecule. Figure 10 shows the emission spectra (λ excitation = 270 nm) of the Methyl Orange (MO) solutions at pH 4 and with different concentrations of: a) AuNPs-Osm b) AuNPs-NaBH₄. The emission spectrum of the MO solution presents two strong emission bands. The band at 290 to 500 nm with a maximum at 330nm correlates with $S_1 \rightarrow S_0$ transitions of the hyper conjugated system of the azobenzene portion of the MO structure. Meanwhile, the band observed between 250 to 288 nm with a maxima at 270 nm, may be attributed to $S_2 \rightarrow S_0$ transitions related to the benzene structure in MO. When gold nanoparticles were added to methyl orange solutions, an increase in the intensity of the fluorescence emission band at 290 to 500 nm was observed, this increase was proportional to the concentration of the nanoparticles in solution. The peak centered at 270 nm presented a more erratic behavior; with the addition of AuNPs-Osm, for concentrations below 2 ppm its intensity decreased relative to the intensity of the MO solution, and for concentrations greater than 2 ppm, its fluorescence intensity increased. For AuNPs-NaBH₄, for most of the samples, the concentration of nanoparticles increased the intensity of this peak compared to the MO solution. It is well known that the fluorescence enhancement or quenching that can be induced by metal nanoparticles relies on two principal mechanisms: the first one is the electromagnetic field enhancement, and the second one is related to the radiation less energy transfer from the fluorophore to the nanoparticles surface area [32]. Therefore, the increase in the signal of MO in the presence of AuNPs may be explained by the stimulation of the MO molecules when they are close to the AuNPs. The active molecules are stimulated through the local electromagnetic field enhancement and are able to induce the

SPR of the AuNPs, creating an energy transfer channel between them.

Although the general trends for both types of nanoparticles are similar, some differences were elucidated in the fluorescence spectra. With the addition of AuNPs-Osm, a slight blue shift of the 290-500 nm peak maxima was observed (from 330 to 320 nm). This trend was proportional to the concentration of the nanoparticles in solution. This blue shift is accompanied by the appearance of a new peak/shoulder between 350-500 nm with a maximum at 360 nm. A similar tendency was observed with AuNPs-NaBH₄, but the peak/shoulder is less defined and has a maximum at a higher wavelength (432 nm). The appearance of the additional peak, near 350-500 nm, was more defined at concentrations of AuNPs near to and higher than 2 ppm for both types of nanoparticles. The correlation of the ratio of the fluorescence intensities of the peaks centered at approximately 330 nm and the appearing shoulder with the concentration of nanoparticles is presented in Figure 11. For both types of nanoparticles the ratio of these peaks (330nm/360nm for AuNPs-Osm and 330nm/340nm for AuNPs-NaBH₄) decreased as the concentration of nanoparticles in solution increased.

These tendencies and the exposed spectral changes are associated with the interaction among MO molecules and AuNPs. An increase of the concentration of gold nanoparticles in the solution may be promoting the formation of Au(MO)_n complexes that give rise to the new PL band. This Au(MO)_n complex should present absorption at an adjacent frequency to the plasmon absorption of gold colloids [33]. Although both types of nanoparticles presented similar behaviors, AuNPs-NaBH₄ produced a more drastic increase in the band related

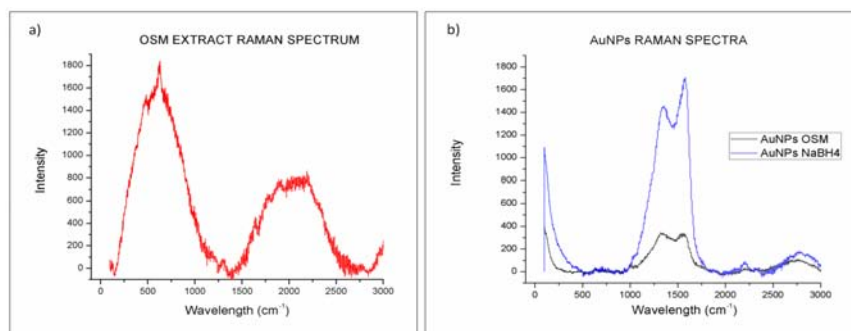


Figure 12: Raman spectra of a) *Osmundaria Obtusiloba* extract and b) AuNPs.

to the hyper conjugated system of MO. It may also be due to entropic factors. AuNPs- NaBH_4 are more homogeneous in nature, all particles are spherical and have smaller size; however, AuNPs-Osm produce a colloidal solution with higher entropy, since it has nanoparticles with four different morphologies, as discussed previously. The higher entropy could be increasing the frequency of collisional quenching in the solution, and as a result produce a decrease in the expected signal. In summary, the major changes in the photoluminescence behavior of AuNPs obtained by different synthesis methods are due to the influence of the following parameters in the fluorescence mechanism: the distance between the fluorophore and the metal nanoparticle, nanoparticle morphology and size, surface modifications, and reaction media.

Surface enhancement raman spectroscopy (SERS) enhancement

SERS analysis was applied to compare the enhancement of gold nanoparticles obtained via biosynthesis with *O. Obtusiloba* and chemical synthesis with NaBH_4 . Figure 12 shows the Raman spectra for AuNPs-Osm, AuNPs- NaBH_4 , and the macroalgae extract. Both types of nanoparticles exhibit the same bands, but AuNPs- NaBH_4 exhibit a higher intensity of the signals. None of the Raman signals generated for the macroalgae extract were present in the AuNPs-Osm spectrograph. The observed peak positions of 4-NTP corresponded to the values reported in the literature [34]. The peak at 1500 cm^{-1} was used to compare the SERS ability of the different AuNPs because it exhibited the highest intensity. The SERS analytical enhancement factors were calculated using equation (2). Due to the fact that SERS Enhancement Factor (EF) is principally affected by the surface adsorbed molecules, it was calculated using a $0.10\text{ }\mu\text{M}$ 4-NTP solution, which was positioned in the linear dynamic range of our calibration curve ($0.05\text{ }\mu\text{M}$ to $1.0\text{ }\mu\text{M}$ $R = 0.998$) A EF of $(1.8 \pm 0.3) \times 10^5$ was determined for AuNPs- NaBH_4 and $(1.3 \pm 0.2) \times 10^5$ for AuNPs-Osm. The observed differences may be due to the diversity of shapes that are present in the AuNPs and the coverage of the colloidal surfaces with the molecule of interest [21].

The nanoparticles produced using the *O. Obtusiloba* extract have mixed morphologies, while nanoparticles obtained using NaBH_4 are all spheres. A more detailed analysis is necessary to determine the ratio of different morphologies in AuNPs-Osm, since Tiwari et al. have reported that the shapes in silver colloids influence their SERS properties [35]. In their study, the intensity of SERS signal was the smallest for silver nanorods. Silver nanospheres had an intermedia

signal, and silver nanoprisms showed the strongest signal.

Conclusion

The synthesis of gold nanoparticles with *Osmundaria Obtusiloba* proved to be an efficient and eco-friendly method. It has significant advantages over traditional methods such as simplicity of the process, elimination of toxic wastes, and potential for scaling up, and is economic viability. The resulting AuNPs have unique properties such as their different morphologies, surface capping, and 10 to 20 nm size ranges. The optical properties of the biosynthesized AuNPs are comparable to the properties of AuNPs obtained through chemical methods. They exhibited a higher quantum yield than the AuNPs synthesized with NaBH_4 , a blue shifted SPR, high UVVIS absorption sensitivity, and SERS. Their difference in optical properties may be credited to their diverse morphology and capping. AuNPs-Osm nanoparticles proved to have excellent optical properties, and as such are suitable candidate for sensing applications. Further optimization of the biosynthesis procedure may be done to favor the formation of some morphology, such as triangles and prisms, which have proven to have more effective SERS signals.

Acknowledgement

This project has been supported by CRES Grant W911NF-11-1-0218, U.S. Department of Defense and by a grant from the Puerto Rico Center of Environmental Neuroscience (PRCEN) NSF Crest Grant HDR-1137725-03. We would like to recognize the Material Characterization Center (MCC) and the Molecular Science Research Building facilities and staff for enabling the use of the instrumentation necessary to performance the AuNPs characterization. Special thanks to the Deanship of Natural Science of UPRRP and the Cornell Center for Materials Research HRTEM facilities for enabling the TEM analysis NSF grant DMR 1120296.

References

- Daniel MC, Astruc D. Gold nanoparticles: assembly, supramolecular chemistry, quantum-size-related properties, and applications toward biology, catalysis, and nanotechnology. *Chem Rev.* 2004; 104: 293-346.
- Faraday M. The Bakerian lecture: experimental relations of gold (and other metals) to light. *Philosophical Transactions of the Royal Society of London.* 1857; 147: 145-81.
- Grzelczak M, Pérez-Juste J, Mulvaney P, Liz-Marzán LM. Shape control in gold nanoparticle synthesis. *Chem Soc Rev.* 2008; 37: 1783-1791.
- Feng H, Yang Y, You Y, Li G, Guo J, Yu T, et al. Simple and rapid synthesis of ultrathin gold nanowires, their self-assembly and application in surface-

- enhanced Raman scattering. *Chem Commun (Camb)*. 2009; 1984-1986.
5. Thakkar KN, Mhatre SS, Parikh RY. Biological synthesis of metallic nanoparticles. *Nanomedicine*. 2010; 6: 257-262.
 6. Zhang Y, Chu W, Foroushani AD, Wang H, Li D, Liu J, et al. New Gold Nanostructures for Sensor Applications: A Review. *Materials*. 2014; 7: 5169-5201.
 7. Kang KA, Wang J, Jasinski JB, Achilefu S. Fluorescence manipulation by gold nanoparticles: from complete quenching to extensive enhancement. *J Nanobiotechnology*. 2011; 9: 16.
 8. Turkevich J, Stevenson PC, Hillier J. A study of the nucleation and growth processes in the synthesis of colloidal gold. *Discussions of the Faraday Society*. 1951; 11: 55-75.
 9. Mulfinger L, Solomon SD, Bahadory M, Jeyarajasingam AV, Rutkowsky SA, Boritz C. Synthesis and Study of Silver Nanoparticles. *Journal of Chemical Education*. 2007; 84: 322.
 10. Mafuné F, Kohno J-y, Takeda Y, Kondow T. Dissociation and Aggregation of Gold Nanoparticles under Laser Irradiation. *The Journal of Physical Chemistry B*. 2001; 105: 9050-9056.
 11. Sun Y, Jose D, Sorensen C, Klabunde KJ. Alkyl and aromatic amines as digestive ripening/size focusing agents for gold nanoparticles. *Nanomaterials*. 2013; 3: 370-392.
 12. Mohanpuria P, Rana N, Yadav S. Biosynthesis of nanoparticles: technological concepts and future applications. *Journal of Nanoparticle Research*. 2008; 10: 507-517.
 13. Sinha S, Pan I, Chanda P, Sen SK. Nanoparticles fabrication using ambient biological resources. *J Appl Biosci*. 2009; 19: 1113-1130.
 14. Kumar V, Yadav SK. Plant-mediated synthesis of silver and gold nanoparticles and their applications. *Journal of Chemical Technology & Biotechnology*. 2009; 84: 151-157.
 15. Arockiya Aarthi Rajathi F, Parthiban C, Ganesh Kumar V, Anantharaman P. Biosynthesis of antibacterial gold nanoparticles using brown alga, *Stoechospermum marginatum* (kützing). *Spectrochimica Acta Part A: Molecular and Biomolecular Spectroscopy*. 2012; 99: 166-173.
 16. Kushnerova TV, Fomenko SE, Kushnerova NF, Sprygin VG, Lesnikova LN, Khotimchenko YS, et al. Antioxidant and membrane-protective properties of an extract from the brown alga *Laminaria japonica*. *Russian Journal of Marine Biology*. 2010; 36: 390-395.
 17. Fujimoto K. Antioxidant activity of algal extracts. Introduction to applied phycology SPB Academic Publishing, The Hague. 1990: 199-208.
 18. Liu X, Atwater M, Wang J, Huo Q. Extinction coefficient of gold nanoparticles with different sizes and different capping ligands. *Colloids Surf B Biointerfaces*. 2007; 58: 3-7.
 19. Fery-Forgues S, Lavabre D. Are Fluorescence Quantum Yields So Tricky to Measure? A Demonstration Using Familiar Stationery Products. *Journal of Chemical Education*. 1999; 76: 1260.
 20. Fletcher AN. Quinine sulfate as a fluorescence quantum yield standard. *Photochem Photobiol*. 1969; 9: 439-444.
 21. Hong S, Li X. Optimal size of gold nanoparticles for surface-enhanced Raman spectroscopy under different conditions. *Journal of Nanomaterials*. 2013; 49.
 22. Haiss W, Thanh NT, Aveyard J, Fernig DG. Determination of size and concentration of gold nanoparticles from UV-vis spectra. *Anal Chem*. 2007; 79: 4215-4221.
 23. Mie G. Articles on the optical characteristics of turbid tubes, especially colloidal metal solutions. *Ann Phys*. 1908; 25: 377-445.
 24. Fernando LM, Merca FE, Paterno ES. Biogenic synthesis of gold nanoparticles by plant-growth-promoting bacteria isolated from philippine soils. *The Philippine Agricultural Scientist*. 2013; 96.
 25. Rajeshkumar S, Malarkodi C, Gnanajobitha G, Paulkumar K, Vanaja M, Kannan C, et al. Seaweed-mediated synthesis of gold nanoparticles using *Turbinaria conoides* and its characterization. *Journal of Nanostructure in Chemistry*. 2013; 3: 1-7.
 26. Stalin Dhas T, Ganesh Kumar V, Stanley Abraham L, Karthick V, Govindaraju K. *Sargassum myriocystum* mediated biosynthesis of gold nanoparticles. *Spectrochimica Acta Part A: Molecular and Biomolecular Spectroscopy*. 2012; 99: 97-101.
 27. Abdelhalim MAK, Mady MM, Ghannam MM. Physical properties of different gold nanoparticles: ultraviolet-visible and fluorescence measurements. *J Nanomed Nanotechnol*. 2012; 3: 2.
 28. Zheng J1, Petty JT, Dickson RM. High quantum yield blue emission from water-soluble Au8 nanodots. *J Am Chem Soc*. 2003; 125: 7780-7781.
 29. Gaiduk A, Ruijgrok PV, Yorulmaz M, Orrit M. Making gold nanoparticles fluorescent for simultaneous absorption and fluorescence detection on the single particle level. *Physical Chemistry Chemical Physics*. 2011; 13: 149-153.
 30. Schaeffer N, Tan B, Dickinson C, Rosseinsky MJ, Laromaine A, McComb DW, et al. Fluorescent or not? Size-dependent fluorescence switching for polymer-stabilized gold clusters in the 1.1-1.7 nm size range. *Chem Commun (Camb)*. 2008; 3986-3988.
 31. Wilcoxon J, Martin J, Parsapour F, Wiedenman B, Kelley D. Photoluminescence from nanosize gold clusters. *The Journal of chemical physics*. 1998; 108: 9137-9143.
 32. Wang Y. Fluorescence Enhancement of Methyl Orange by Silver Nanoparticles. *Advanced Materials Research*. 2013.
 33. Zhang A, Fang Y. Influence of adsorption orientation of methyl orange on silver colloids by Raman and fluorescence spectroscopy: pH effect. *Chemical Physics*. 2006; 331: 55-60.
 34. Abdelsalam M. Surface enhanced raman scattering of aromatic thiols adsorbed on nanostructured gold surfaces. *Open Chemistry*. 2009; 7: 446-453.
 35. Tiwari VS, Oleg T, Darbha GK, Hardy W, Singh J, Ray PC. Non-resonance SERS effects of silver colloids with different shapes. *Chemical Physics Letters*. 2007; 446: 77-82.